

## Facile Synthesis of Hierarchical Alumina Monoliths with Tubular Macropores and Ordered Mesoporous Walls

Kuibao Zhang,<sup>1</sup> Zhengyi Fu,<sup>\*1</sup> Jinyong Zhang,<sup>1</sup> Tadachika Nakayama,<sup>2</sup> Koichi Niihara,<sup>2</sup> and SooWohn Lee<sup>3</sup>

<sup>1</sup>State Key Laboratory of Advanced Technology for Materials Synthesis and Processing,  
Wuhan University of Technology, Wuhan 430070, P. R. China

<sup>2</sup>Extreme Energy-Density Research Institute, Nagaoka University of Technology, 1603-1 Nagaoka, Niigata 940-2188

<sup>3</sup>Department of Materials Engineering, SunMoon University, Asan, ChungNam 336-708, Korea

(Received June 15, 2010; CL-100562; E-mail: zyfu@whut.edu.cn)

A facile approach of evaporation-induced self-assembly plus coating was developed using nonwoven fabrics (NF) as a sacrificial scaffold, leading to the acquisition of hierarchically macro/mesoporous alumina monolith. The macropores templated by NF show a tubular structure of about 10  $\mu\text{m}$  in channel diameter. The monolith is composed of ordered mesostructured wall with large-sized mesopores and high thermal stability. The regularity of the mesopores can be maintained up to 900  $^{\circ}\text{C}$ , even after the amorphous  $\text{Al}_2\text{O}_3$  transforms to crystalline structure ( $\gamma\text{-Al}_2\text{O}_3$ ). This facile route can be extended to the preparation of other hierarchically macro/mesoporous monoliths such as  $\text{TiO}_2$ ,  $\text{ZrO}_2$ ,  $\text{ZnO}$ , et al.

The incorporation of macropores in mesoporous structures is of great interest in recent years because the hierarchically macro/mesoporous materials are efficient for the treatment of bulky molecules and transportation of guest species to framework binding sites, which can find substantial applications in catalysis, sorption, and separation.<sup>1–3</sup> The first report of ordered macro/mesoporous material was produced by Yang and co-workers in the synthesis of hierarchically porous silica.<sup>4</sup> Compared with a pure siliceous counterpart, nonsiliceous mesoporous materials are more versatile, and considerable efforts have been devoted in the last decade.<sup>5–7</sup> Mesoporous alumina (MA) is one of the most important nonsiliceous mesoporous materials with popular industrial applications in catalysis, catalysis support, and other fields.<sup>8</sup> Unfortunately, mesoporous alumina is usually obtained with wormhole-like mesopores because of its fast hydrolysis–condensation rate.<sup>9</sup> The synthesis of ordered mesoporous alumina framework has been proved even more challengeable when incorporated with macropores.<sup>10</sup>

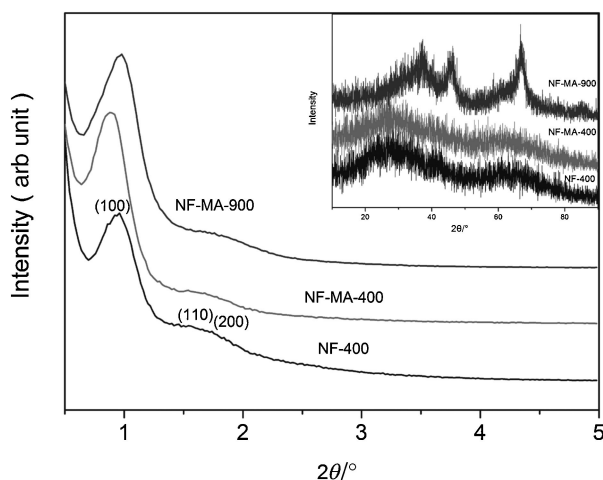
Recently, Yuan et al.<sup>11</sup> provided a facile route of evaporation-induced self-assembly (EISA) to synthesize ordered mesoporous  $\gamma\text{-Al}_2\text{O}_3$  with high thermal stability. On this basis, Dacquin et al.<sup>12</sup> introduced monodispersed latex spheres of polystyrene bead as the macropore template to synthesize highly organized macro/mesoporous alumina particles. More recently, Li et al.<sup>13</sup> reported the synthesis of hierarchical  $\gamma\text{-Al}_2\text{O}_3$  monoliths with highly ordered 2D hexagonal mesopores in macroporous walls using PU foam as the sacrificial macropore skeleton. Herein, we proposed a facile preparation of macroporous alumina monoliths with tubular macropores and ordered mesoporous walls using improved EISA plus coating technology, in which nonwoven fabrics (NF) were utilized as the macropore sacrificial skeleton. PU foam was also employed as the macropore template for comparison according to ref 13.

Pluronic P123 ( $M_{\text{av}} = 5800$ ,  $\text{EO}_{20}\text{PO}_{70}\text{EO}_{20}$ ) and aluminum isopropoxide were purchased from Aldrich. Nonwoven fabrics were bought from Beijing Xinlong Corporation. In a typical synthesis, 0.9 g of P123 was dissolved in 20 mL of ethanol at room temperature with vigorous stirring for 3 h. Then 1.5 mL of 67 wt % nitric acid and 2.04 g of aluminum isopropoxide were added into the above transparent solution. The solution was covered with PE film and stirred at room temperature for about 5 h. A piece of nonwoven fabric was immersed in the above solution and aged at 25  $^{\circ}\text{C}$  for 24 h. Then the NF immersed sol was placed in a 60  $^{\circ}\text{C}$  drying cabinet for solvent evaporation. After 2 days of evaporation and drying, the MA-coated NF became a light yellow monolith with a degree of mechanical strength. Calcinations were carried out at 400  $^{\circ}\text{C}$  for 4 h with a heating rate of 1  $^{\circ}\text{C min}^{-1}$  and an atmosphere of flowing air. For calcination at higher temperature, the sample was first calcined at 400  $^{\circ}\text{C}$  for 4 h and then heated to the destined temperature with a rate of 10  $^{\circ}\text{C min}^{-1}$  and holding time of 1 h.

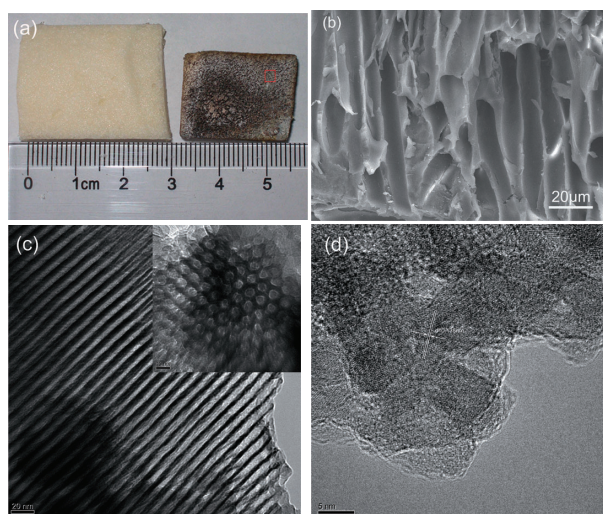
Powder X-ray diffraction of wide angle (10–90 $^{\circ}$ ) and small angle (0.5–5 $^{\circ}$ ) were conducted using a Rigaku Ultima III diffractometer with  $\text{Cu K}\alpha$  radiation. The microstructure and pore diameters were observed by scanning electron micrographs (SEM, Hitachi S-3400N) and transmission electron micrographs (TEM, JEOL JEM-2100F). Nitrogen physisorption measurements were performed at 77 K on a Micromeritics ASAP2020 instrument. The Brunauer–Emmett–Teller (BET) calculations of surface area and Barrett–Joyner–Halenda (BJH) calculations of pore volume and pore size distribution were performed on the desorption branches of the isotherms.

Figure 1 presents the small-angle and wide-angle (inserted) X-ray diffraction spectra of a sample prepared from direct EISA (MA-400) and samples with NF incorporated as the macropore skeleton (NF-MA-400 and NF-MA-900). The small-angle X-ray spectra (SAXS) confirm the ordered mesoporous structure of all the three samples.<sup>14,15</sup> The SAXS of MA-400 shows several well-resolved peaks, which can be indexed as (100), (110), and (200) Bragg reflections of  $p6m$  space group.<sup>10</sup> The structural regularity remains nearly invariable when NF is incorporated in NF-MA-400. The ordered mesoporous structure is maintained even after it was calcined at 900  $^{\circ}\text{C}$ . The wide-angle XRD indicates that both MA-400 and the NF-MA-400 are composed of totally amorphous walls. However, this amorphous structure transforms to crystalline  $\gamma\text{-Al}_2\text{O}_3$  (see NF-MA-900 in Figure 1) when it is calcined at 900  $^{\circ}\text{C}$  for 1 h. The ordered mesoporous MA with crystalline wall is rarely obtained and definitely provides this material with high thermal stability.<sup>12</sup>

Figure 2a shows the morphology comparison of the as-synthesized MA-coated NF monolith and the monolith after



**Figure 1.** Small-angle and wide-angle (inserted) X-ray diffraction spectra of MA-400, NF-MA-400, and NF-MA-900.



**Figure 2.** (a) Optical image of the sol-coated NF monolith before and after 400 °C calcination, (b) SEM image of NF-MA-400, (c) TEM images of NF-MA-400, and (d) HRTEM image of NF-MA-900.

calcination at 400 °C. The as-synthesized monolith exhibits a light-yellow color similar to pure MA solid reported by Yuan et al.<sup>11</sup> The sample retains the monolithic state after being calcined at 400 °C, and obvious shrinkage of about 26% in linear dimensions can be observed. The framework of the NF-MA-400 monolith was further inspected by SEM as shown in Figure 2b. An interconnected macroporous framework is observed with tubular macropores of about 20 μm in diameter. The formation of tubular macropores is associated with the NF sacrificial scaffold. The P123-directed aluminum supramolecular group was coated on the fabric when it was immersed in the alumina precursor contained solution. The macropore template (NF) was gradually eliminated under calcination, leading to the formation of tubular pores at the location of NF fabrics. The diameter of the tubular pores can be modified by choosing different kinds of nonwoven fabrics.

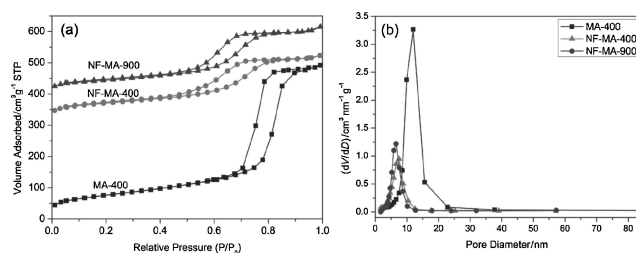


**Figure 3.** (a) N<sub>2</sub> isotherms of MA-400, NF-MA-400, and NF-MA-900 and (b) corresponding BJH pore size distribution derived from the desorption branches of the isotherms.

Figure 2c reveals the refined microstructure of the NF-MA-400 sample under TEM observation. Stripe-like domain is observed from the (110) direction, which is actually mesosized channels parallelly aligned to each other. Inset in Figure 2c shows the mesostructure observed from the (001) direction, which directly reveals the 2D hexagonal mesopores arranged in a high regularity. This morphology further confirms that the macrosized channels are connected with ordered mesoporous walls. The ordered mesostructure can be maintained up to 900 °C as indicated by both SAXS and TEM characterizations (TEM not shown here). For the 900 °C calcined sample, high-resolution TEM image (Figure 2d) reveals the existence of several crystalline particles with distinct lattice fringes. The spacing of the lattice fringe is estimated to be 0.139 nm, which is in accordance with the (440) lattice plane of  $\gamma$ -Al<sub>2</sub>O<sub>3</sub>.

N<sub>2</sub> physisorption isotherms exhibit typical type IV curves with H1-shaped hysteresis loops in all the three samples, indicating their uniform cylindrical mesopores (Figure 3a).

The physisorption measurements reveal a high BET surface area and a pore volume, 270 m<sup>2</sup> g<sup>-1</sup> and 0.75 cm<sup>3</sup> g<sup>-1</sup>, for the MA-400 sample.<sup>14</sup> When the macropore scaffold is introduced for NF-MA-400 and NF-MA-900, the BET surface area and pore volume decreased to 183, 159 m<sup>2</sup> g<sup>-1</sup> and 0.30, 0.33 cm<sup>3</sup> g<sup>-1</sup>, respectively. The connections among the macropores and mesopores take up a large amount of the surface area, leading to the decrement of mesopore volume as well as the total surface area. Figure 3b presents the BJH pore-size distributions derived from the desorption branches of the isotherms. The MA-400 shows mesopores having a diameter of around 9.9 nm, while the NF-MA-400 and NF-MA-900 show smaller mesopores of 6.0 and 6.3 nm. The pore size obtained from physisorption is in agreement with that observed from TEM images. Further calcinations at higher temperatures exhibit little effect on the pore size distribution, which once again reveals its good thermal stability.

From the above results, the preparation of hierarchically macro/mesoporous alumina monoliths undergoes four steps: sol preparation, impregnation, solvent evaporation, and calcination. To obtain highly ordered mesoporous sol precursor, the key factors include suitable selection of aluminum source and strict control of water concentration.<sup>9,11</sup> The calcination process is also vital for the preparation of ordered macro/mesoporous alumina monolith. When the MA-coated PU foam was directly calcined in a muffle furnace under flowing air, only disordered mesoporous particles can be obtained.<sup>13</sup> The ordered mesostructure disappeared and the macroporous monolith collapsed.

This may be due to the removal of P123 and PU foam occurring at almost the same temperature. The intensive reaction of PU foam and O<sub>2</sub> would ultimately destroy the P123-directed regular mesostructure. In this letter, two-step calcination was employed, first in a tubular furnace under flowing Ar and then in a muffle furnace with flowing air, to eliminate P123 and PU foam separately. Then the ordered mesostructure was retained and the monolith with macroporous architecture was preserved. From a catalytic perspective, the high thermal stability will definitely provide the novel hierarchically macro/mesoporous  $\gamma$ -Al<sub>2</sub>O<sub>3</sub> monolith with broad applications.<sup>16</sup>

In summary, a macroporous alumina monolith with ordered mesoporous walls was prepared by a facile EISA plus coating route with nonwoven fabric (NF) as the macropore sacrificial scaffold. These materials show high thermal stability and narrow pore size distribution. The macroporous structure can be obtained using other sacrificial scaffold (e.g., PU foam), and this route can be expanded to the preparation of other hierarchically macro/mesoporous monoliths such as TiO<sub>2</sub>, ZrO<sub>2</sub>, ZnO, et al.

The authors would like to acknowledge the financial support by the National Natural Science Foundation of China (NNSFC) under granted No. 50772081 and No. 50821140308, and the Ministry of Education of China under granted No. PCSIRT0644.

## References

- I. Soten, G. A. Ozin, *Curr. Opin. Colloid Interface Sci.* **1999**, *4*, 325.
- C. F. Blanford, H. Yan, R. C. Schroden, M. Al-Daous, A. Stein, *Adv. Mater.* **2001**, *13*, 401; D. Grosso, G. J. de A. A. Soler-Illia, E. L. Crepaldi, B. Charleux, C. Sanchez, *Adv. Funct. Mater.* **2003**, *13*, 37; X.-Y. Yang, Y. Li, G. V. Tendeloo, F.-S. Xiao, B.-L. Su, *Adv. Mater.* **2009**, *21*, 1368.
- D. M. Antonelli, *Microporous Mesoporous Mater.* **1999**, *33*, 209; J.-L. Blin, A. Léonard, Z.-Y. Yuan, L. Gigot, A. Vantomme, A. K. Cheetham, B.-L. Su, *Angew. Chem., Int. Ed.* **2003**, *42*, 2872; Z.-Y. Yuan, T.-Z. Ren, B.-L. Su, *Adv. Mater.* **2003**, *15*, 1462.
- P. Yang, T. Deng, D. Zhao, P. Feng, D. Pine, B. F. Chmelka, G. M. Whitesides, G. D. Stucky, *Science* **1998**, *282*, 2244.
- D. M. Antonelli, J. Y. Ying, *Angew. Chem., Int. Ed. Engl.* **1996**, *35*, 426; P. Yang, D. Zhao, D. I. Margolese, B. F. Chmelka, G. D. Stucky, *Chem. Mater.* **1999**, *11*, 2813; B. Tian, X. Liu, B. Tu, C. Yu, J. Fan, L. Wang, S. Xie, G. D. Stucky, D. Zhao, *Nat. Mater.* **2003**, *2*, 159.
- R. Ryoo, S. H. Joo, S. Jun, *J. Phys. Chem. B* **1999**, *103*, 7743; S. H. Joo, S. J. Choi, I. Oh, J. Kwak, Z. Liu, O. Terasaki, R. Ryoo, *Nature* **2001**, *412*, 169.
- P. Y. Feng, Y. Xia, J. L. Feng, X. Bu, G. D. Stucky, *Chem. Commun.* **1997**, 949; L. M. Wang, B. Z. Tian, J. Fan, X. Liu, H. Yang, C. Yu, B. Tu, D. Zhao, *Microporous Mesoporous Mater.* **2004**, *67*, 123; X. He, D. Antonelli, *Angew. Chem., Int. Ed.* **2002**, *41*, 214.
- J. Cejka, *Appl. Catal., A* **2003**, *254*, 327; C. Boissière, L. Nicole, C. Gervais, F. Babonneau, M. Antonietti, H. Amenitsch, C. Sanchez, D. Grosso, *Chem. Mater.* **2006**, *18*, 5238.
- Z. Zhang, T. J. Pinnavaia, *J. Am. Chem. Soc.* **2002**, *124*, 12294; K. Niesz, P. Yang, G. A. Somorjai, *Chem. Commun.* **2005**, *15*, 1986.
- O. Sel, D. Kuang, M. Tommes, B. Smarsly, *Langmuir* **2006**, *22*, 2311.
- Q. Yuan, A.-X. Yin, C. Luo, L.-D. Sun, Y.-W. Zhang, W.-T. Duan, H.-C. Liu, C.-H. Yan, *J. Am. Chem. Soc.* **2008**, *130*, 3465.
- J.-P. Dacquin, J. Dhainaut, D. Duprez, S. Royer, A. F. Lee, K. Wilson, *J. Am. Chem. Soc.* **2009**, *131*, 12896.
- L.-L. Li, W.-T. Duan, Q. Yuan, Z.-X. Li, H.-H. Duan, C.-H. Yan, *Chem. Commun.* **2009**, 6174.
- T. Sen, G. J. T. Tiddy, J. L. Casci, M. W. Anderson, *Angew. Chem., Int. Ed.* **2003**, *42*, 4649.
- C. F. Xue, B. Tu, D. Y. Zhao, *Adv. Funct. Mater.* **2008**, *18*, 3914.
- S. F. J. Hackett, R. M. Brydson, M. H. Gass, I. Harvey, A. D. Newman, K. Wilson, A. F. Lee, *Angew. Chem., Int. Ed.* **2007**, *46*, 8593.